Particle transport mechanism in liquid-liquid-solid multiphase pipeline flow of high viscosity oil-water-sand

Archibong Archibong-Eso[1, *], Yahaya Baba[2], Aliyu Aliyu[3], Joseph Ribeiro[5], Fidelis Abam[6], Hoi Yeung[4]

[1]Department of Mechanical Engineering, University of Birmingham, Dubai, UAE
[2]Department of Biological and Chemical Engineering, Sheffield University, UK
[3]School of Computing and Engineering, University of Huddersfield, UK
[4]Oil & Gas Engineering Centre, Cranfield University, Bedfordshire, UK
[5]Department of Petroleum Engineering, Kumasi Technical University, Ghana
[6]Energy, Exergy and Environment Research Group, Michael Okpara University of Agriculture, Nigeria

Abstract

In this study, investigation of sand transport in heavy oil-water multiphase flow is carried out. The study is conducted in three multiphase flow pipeline test facilities with internal diameters (ID) of 1, 1 and 3 inches. The pipeline orientation relative to the horizontal in the facilities are 0˚, +30˚ and 0˚ respectively. Oil viscosity of 3.5 and 10.0 Pa.s with sand volume fraction from 0.010 – 0.100 vol/vol are used in the study. The effect of oil viscosity, upward inclination, sand volume fraction, pipe internal diameter and water cut on sand transport mechanism in pipelines are investigated. In the horizontal test section, flow patterns namely: Dispersed Flow (DF), Plug Flow (PF), Plug Flow with Moving Sand Bed (PFM) and Plug Flow with Stationary Sand Bed (PFS) were identified through flow visualization. In addition to the aforementioned, two flow patterns; the Stratified Wavy Flow with Moving Sand Bed (SWM) and Stratified Wavy Flow with Dunes, (SWD) were observed in the inclined pipeline orientation. Pressure gradient measured, decreased with a decrease in water cut until a minimum value is reached. Beyond the minimum pressure gradient, further reduction in water cut led to an increase in pressure gradient. Sand Minimum Transport Condition (MTC) in the oil-water-sand test were largely the same for the 1-inch 30° upward inclined and the 1-inch horizontal test section while that of the 3-inch horizontal test section was considerably higher. An improved MTC predictive correlation is proposed for multiphase heavy oil-water-sand flow. Proposed correlation outperforms existing model when tested on the heavy oil-water-sand dataset.

Highlights

- Experimental investigations of concurrent high viscosity oil, water, and sand (high viscosity oil-water-sand) multiphase flow in pipelines is presented
- Evaluation of existing models' predictive capability in high viscosity oil-water-sand multiphase flow

*Corresponding Author: A. Archibong-Eso
 Email address: a.e.archibong@bham.ac.k

- Investigate the effect of an upward 30 degree inclined pipeline orientation and an increase in pipe internal diameter on sand minimum transport condition (MTC).
- Comparatively evaluate pressure gradient characteristics of water-sand and oil-water-sand multiphase flow
- Propose an improved predictive correlation for MTC of sand in high viscosity oil-water-sand multiphase flow in horizontal pipelines.

1 Introduction

Three-phase oil–water–sand flow in pipelines are prevalent during crude oil production. These flows are encountered when water is used to assist the production and transport of unconventional crude oil resources such as heavy oils and bituminous sand. Numbers released by the British Petroleum's statistical review of world energy 2019 report (BP, 2019) shows that the world's primary energy consumption grew by 2.9% from 2018. This is the steepest growth since 2010. Conventional crude oil resources have been significant contributor to global energy consumption. In addition, the report indicates that the year-on-year increase in world energy demand is in its tenth consecutive year. This trend together with advancement in technology, growth in developing economies, and increasing world population, is partly responsible for accelerating depletion of conventional oil reserves. Amidst this depletion, consumption has outpaced production and is fast surpassing the pre-world economic depression figures. One way the oil and gas industry uses to replenish depleting conventional reserves and thus satisfy the world energy demand, is the exploration and production of unconventional resources. Heavy oil is a standout candidate amongst unconventional resources because of reasons including technological advances, availability of large reserves (70% of world oil reserves are constituents of heavy oil) and geopolitics.

Heavy oils are characterised by their high viscosity (>0.1 Pa.s) and low API gravity (<22° API), these attributes is due to the presence of asphaltenes which may constitute of up to 50% by weight in some resource. They are generally dense and viscous in nature (similar to molasses) with some impurities. Due to its peculiar characteristics, heavy oil can be difficult to economically produce and transport. It therefore becomes important for the right technology to be developed and deployed for its production and transportation.

Some producers in Canada, Venezuela and the United States use a promising production technique - Cold Heavy Oil Production with Sand (CHOPS) - a technique that encourages the production of heavy crude oil with sand. Co-producing heavy crude oil with sand has several attendant issues such as handling cost for sand (and its disposal), producing wells workover as a result of accumulated sand in the wellbore and downhole pumps, increased wear due to the presence of sand in the produced fluids etc. (Wagg et al. 2009). To curtail these disadvantages which has militated CHOPS implementation and to ensure producers increase its return on investment; production, transportation and

processing facilities with capabilities of handling sand is imperative. The design, operation and control strategies of such facilities must account for sand presence in the produced well fluids. To achieve the aforementioned, an understanding of sand transport mechanism in high viscosity oil-water-sand is essential.

Some three phase studies available in the literature are the works of Karami *et al.,* (2016) also conducted experimental study using 3-phase facility with 6-in.-inner- diameter (ID) facility to investigate characteristics of three-phase stratified wavy flow in horizontal pipelines. The flow characteristic they investigated are wave pattern, liquid holdup, water holdup, pressure gradient, and wetted-wall fraction. Experimental data acquired were compared with predictions obtained from a transient multiphase-simulation software. Results obtained from simulation were in agreement with experiments for measured liquid-holdup and pressure-gradient data. However, the three-phase water-holdup trends were under predicted. Mathew *et al.*, (2001) performed solid transport experiment on the BP Amoco 6-in multiphase flow test facility using several fluids including: water, oil, and carboxymethylcellulose solutions. Viscosity of the fluids used ranged from 0.15 – 0.3 Pa.s. The authors noted in slug flow, water and low-viscosity oil were able to transport the sand uphill, high-viscosity solution on the other hand was unable to transport the solids. The feature was examined in comparison to the model for solids transport in near-horizontal Pipes.

However, most studies in literature on solids transport related to the petroleum industry are conducted using low viscosity liquid and were mostly limited to two-phase liquid-solid flow. Recently, some of such studies include Chen et al. (2020), Archibong-Eso et al. (2020), Fajemidupe et al (2019a), Fajemidupe et al. (2019b), Okeke et al. (2019), Yang et al. (2019) and Leporini et al. (2019).

Crowe (2005) characterized the flow of solid particles in single phase liquid flow into: dispersed, scouring, moving dunes and stationary bed.

- Stationary Bed: Stationary bed was observed at very low liquid velocity; immobile sand particles form stationary bed with a flat surface at the bottom of the pipe. If the liquid velocity is increased, sand particles attain stable bed height with the particles at the top of the bed moving downstream thus increasing the bed's length. (Archibong 2015)

- Moving Dunes: Sand bed breaks up into moving dunes on increasing the liquid velocity in stationary bed flow patterns, the grains at the dunes surface are rolled along by the liquid from back to front. The grains falls in sheltered regions in front of the dune and the dune passes over the particles until they are once again on the top surface (Yan 2010).

- Scouring: Sand particles on top of the dune's surface in the moving dunes flow pattern, roll along with increased momentum as a result of increase in liquid velocity. Increased momentum ensures that the particles goes further downstream beyond the sheltered region and are swept away as individual scouring grains.

- Dispersed: At very high liquid velocity, sand particles pickups its highest momentum and becomes dispersed in the flow in a random and chaotic pattern. The degree of homogeneity of the particles in the liquid is a function of the liquid velocity.

Research work on oil-water-solid flow in literature is sparse, a fortiori, viscous oil-water-solid flow. Multiphase flow research community have paid little attention to this study. Heavy oil-gas two-phase flow has gained researchers interest in the past 10-15 years due to interest shown by the oil and gas industry to the exploration and production of heavy oil fields. Some of such studies include Archibong-Eso et al. 2014, 2015, 2017, 2018 and 2019, Baba et al. 2017, 2018, 2019, Al-Safran 2016 and 2018, Zhao 2013 amongst others.

In comparison, high viscosity liquid-liquid-solid three-phase flow has not gained similar interest. Few studies exist in literature for three-phase oil-water-sand flow. Gillies et al. (1995) studied oil-water-sand flow in horizontal pipes. Oil and water with viscosities of 0.066 and 0.01 Pa.s respectively were used as liquid phases. The authors reported a washing out of sand from oil when water was introduced into the oil-sand system in the pipeline. Considerable reduction in pressure gradient was reported. Notably, oil viscosity in their study was low and no information on MTC or flow patterns were presented.

McKibben et al. (2013) conducted a study on water-assisted pipeline transported of heavy oil with sand. Their work was carried out the Saskatchewan Research Council (SRC) under the aegis of a consortium of Canadian heavy-oil producers. To the authors' knowledge, this study is the only study in literature that was conducted for high viscous oil-water-sand three-phase flows. Oil used in the study to simulate heavy crude oil has viscosity ranging from 0.2 – 31.4 Pa.s. Sand volume fraction of 6 and 12%, with pipeline IDs of 0.05, 0.1 and 0.2 m were used in the study. The authors reported that sand transport in multiphase flow reduced with increase in water cut and reduction in viscosity. They defined water cut as the ratio of the water superficial velocity to the mixture velocity, i.e.: $wc = V_{sw}/V_m$ (generally, superficial velocities are notional velocities of fluid which is calculated as if the given phase or fluid were the only one flowing or present in a given cross sectional area). A sand transport model for the prediction of the minimum velocities required for water-assisted deposit free oil-water-sand flow was developed by comparing the friction velocity V^* that provides a suitable measure of the magnitude of turbulence in a pipeline to the terminal settling velocity, V_∞ (McKibben et al. 2013). McKibben et al.

151   (2013) stated that the correlation provided reasonable estimates of the pressure gradient
152   in high viscous oil-water flow.

153   The mixture friction factor correlation proposed by McKibben et al. (2013) for mixture is
154   given by:

$$f_m = 15 \cdot Fr^{-0.5} f_w^{1.3} f_o^{0.32} C_w^{-1.2}$$

155   Froude number, Fr, mixture friction factor for the aqueous phase, f_w and oil friction factor,
156   f_o are defined by:

$$Fr = \frac{V_M}{\sqrt{gD}} > 0.35$$

$$f_w = \frac{1}{\sqrt{16 \log \sqrt{5.7/\rho_m V_M^2 D}}}$$

$$f_O = \frac{16}{Re}; \; Re = \rho_o V_m D / \mu_w$$

157

158   The above correlations were only valid for the water-assisted flow region, Froude number,
159    $Fr > 0.35$. For $Fr \leq 0.35$, flow was considered to be non-water assisted.

160   To enhance understanding of sand transport mechanism, which is vital in pipeline design,
161   maintenance and in crude oil production & transportation, this study experimentally
162   investigates three-phase high viscous oil-water-sand flow. This study will help inform
163   production and transportation strategy for high viscosity crude oils fields. In addition, it
164   could help improve the maintenance, control and design of pipelines and unit operations
165   equipment used in heavy oil exploration and production.

166 2 Materials and methods

167   In this section, description of the fluids (heavy oil and water), solids (sand), measuring
168   devices/equipment are presented. A general description (with aid of schematics) of the
169   high viscosity multiphase flow test facilities used in the study are presented. This test
170   facility have been used by (Aliyu et al., 2017; Archibong-Eso et al., 2018; Baba et al.,
171   2017b, 2017a, 2018).

2.1 Test materials

Sand particles, branded as Congleston HST 95 are used in this study with physical properties stated by manufacturer's specification thus: density, 2650 kg/m³ and mean particle size of 150 microns. From manufacturer's specification sheet, the d_{10}, d_{50} and d_{95} of the sand particles were 100, 144 and 210 microns respectively as shown in Figure 1. These test particles were chosen because it was similar to properties of sand particles found in most oil and gas production fields. Laboratory tests of particle distribution analysis using sieve techniques was used to validate d_{10}, d_{50} and d_{95} of the sand particles stated by manufacturers. This technique involves the weighing of sand from a particular sample and passing them through sieves (screens) of decreasing sizes.
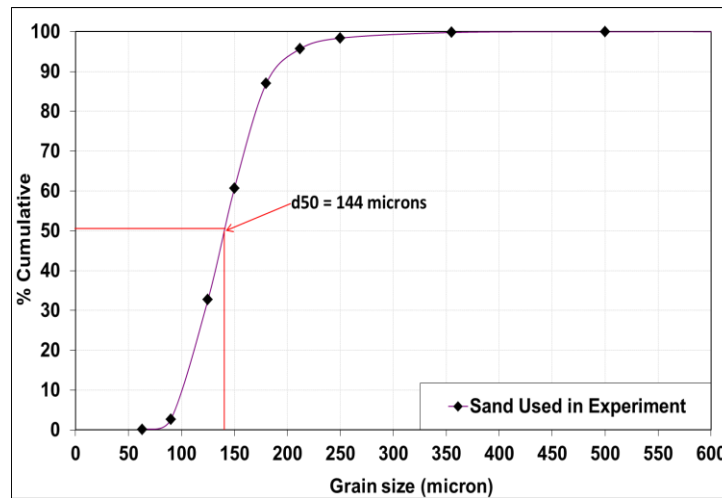
Figure 1: Particle Sand Distribution for HST 95

The screens are mounted on the sieve shakers. Horizontal and vertical motion is applied to the sieves to enhance particles movement. The quantity of particles remaining in each sieve is weighed, and subtracted from the weight of the empty sieve. Results obtained are used in particle size distribution analysis as shown in Figure 1.

Water and mineral oil were used as the test liquids in this experimental investigation. CYL 680 manufactured by Total UK were used in this study. Physical properties obtained from manufacturer's specification (and validated by laboratory measurements using Brookfield DV-I™ prime viscometer) are shown in Table 1. Water used was from the public water supply to Cranfield University.

**Table 1: Properties of test liquids at 25°C**

Test fluids	Density (kg/m³)	Viscosity (Pa.s)	Interfacial tension (N/m)	API gravity[1]
Water	≈998	0.001	0.029	--
CYL680	≈ 918	0.90 − 8.00		22.67

[1]API gravity, $API = \frac{141.5}{SG} - 131.5$, $SG = \frac{\rho_{oil@25°C}}{\rho_{water@25°C}}$ $SG = specific\ gravity$

## 2.2 Experimental test rigs

Two flow loops with different pipe internal diameters were used for horizontal high-viscous oil-water-sand three-phase studies. In addition, a 30° upward inclined flow loop was used to study the effect of upward inclination on the three-phase flow. All the facilities are situated at the Oil and Gas Engineering Centre, Cranfield University, UK. The inclined facility operates in the same fashion and have the same operating equipment as the 1-inch horizontal facility differing only in the main test section inclined orientation. Similarly, the 3-inch facility differ from the 1-inch facility in length and pipe internal diameters. The 1-inch horizontal, 1-inch inclined and 3-inch horizontal facilities have main test sections of 5.5 m, 8.0 m and 17.7 m as can be seen schematically represented in Figure 2 and Figure 3 respectively.
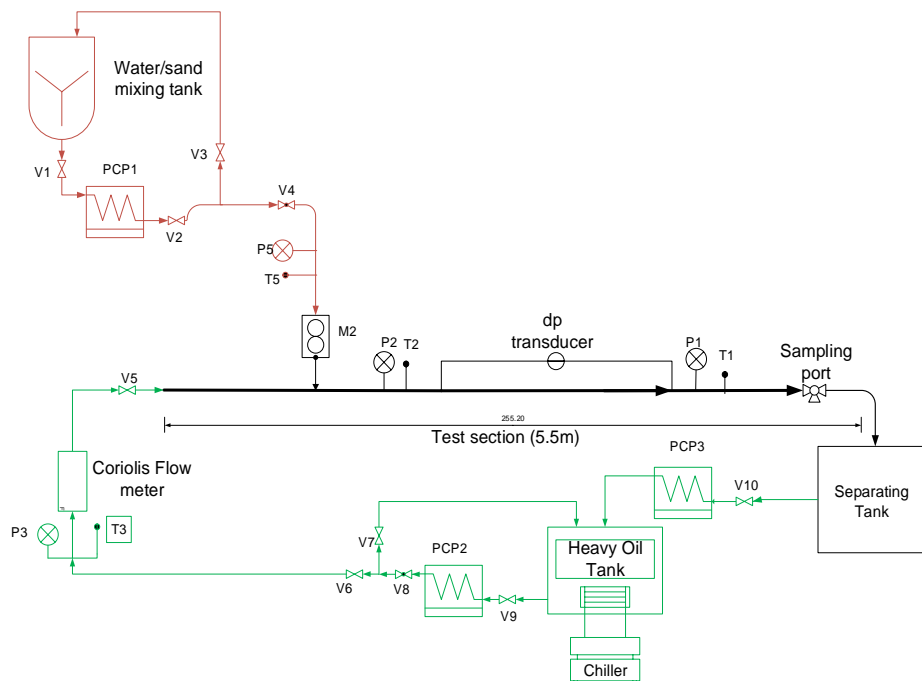
Figure 2: Schematic of the 1-inch multiphase flow facility (Length of main test section are 5.5 m and 8.0 m in the horizontal and inclined orientations respectively).
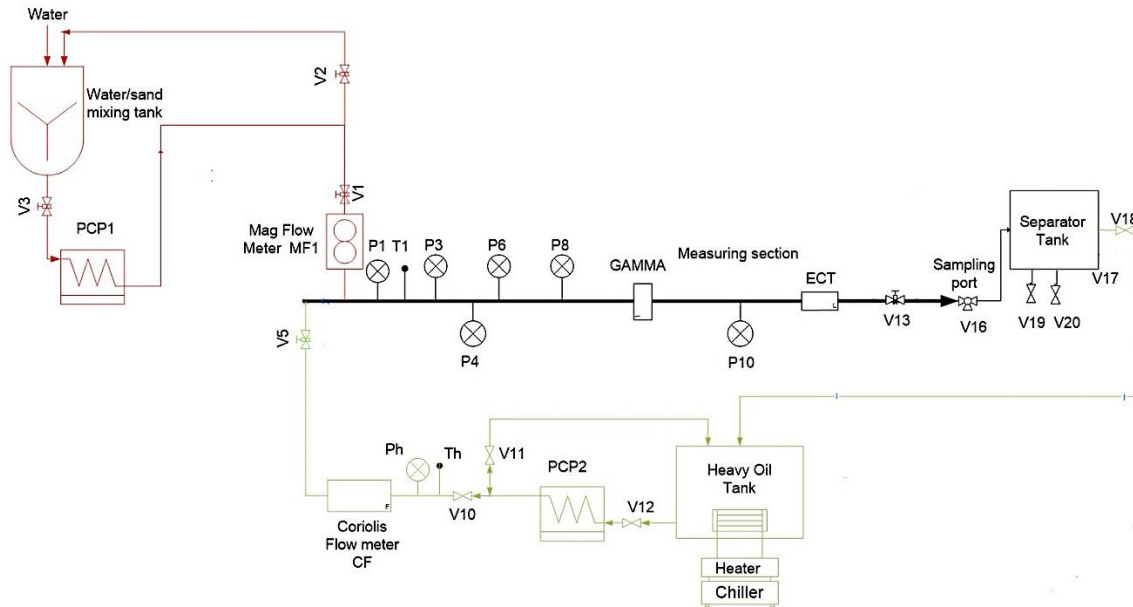
209

210   **Figure 3: Schematic of the 3-inch multiphase flow facility, (length of main test section is 17.7 m).**

211   ## 2.2.1 Slurry System (water-sand)

212   Water-sand (slurry) system consists of a 0.2 m^3 cylindrical plastic vessel with a maximum
213   allowable sand volume fraction of 0.15 volume by volume. An axial flow impeller with twin
214   blades placed about 0.3 m above the vessel's conical base is used to stir the slurry for
215   mixture homogeneity. The conical base opens into a polyvinyl chloride (PVC) pipe that is
216   connected to the suction of the slurry pump, a progressive cavity pump (PCP). The PCP
217   has a maximum flowrate 0 – 2.18 m^3/hr and discharge pressure of 10 bara, the PCP
218   pumps the slurry into the test line via a Promag 55S50, DN50 electromagnetic flowmeter
219   with maximum flow rate of 2.18 m^3/hr. A 4 – 20 mA HART output is used for data
220   acquisition and logging. The 1-inch inclined test section utilizes the same unit operations
221   equipment. For the 3-inch facility, the setup differs in that the cylindrical mixing vessel
222   manufactured from a steel material has a capacity of 2.5 m^3 with a three-blade axial
223   impeller used to stir the slurry mixture for homogeneity. The vessel's conical base opens
224   into the slurry pump; a PCP with discharge pressure of 16 barg, the PCP pumps the slurry
225   into the test line via a Promag 55S800 DN80 electromagnetic flowmeter with maximum
226   flowrate 20 m^3/hr.

227   ## 2.2.2 Oil System

228   A 0.15-m^3 plastic tank capacity insulated on the periphery was used to store oil in the 1-
229   inch horizontal facility. A variable speed PCP with maximum capacity of 0.72 m^3/hr is
230   used in pumping oil. Endress+Hauser's Promass 831 DN 50, a Coriolis flowmeter, with
231   range, 0 – 180 m^3/hr is used in oil metering. The flowmeter has three outputs; mass flow
232   rate, density and viscosity. The HART output from the meter is 4 – 20 mA is connected
233   to a data acquisition system for data logging during experimental runs using the LabVIEW

8

version 8.6.1 software. The 1-inch inclined facility utilizes the same unit operation equipment. In the 3-inch test facility, mineral oil is stored in a 2 m³ capacity steel tank. A variable speed PCP with maximum capacity 17 m³/hr, is used in pumping oil. A Promass 831 DN 80, Coriolis flowmeter with range 0 – 171 m³/hr, manufactured by Endress+ Hauser is used in oil metering.

2.2.3 Multiphase Separation System

Gravity driven separators are used to separate oil-water-sand multiphase mixture at the end of experiment. The separation system consists of a primary and secondary separator. For the 1-inch inclined and horizontal facilities, the primary separator is a rectangular shaped plastic tank with a viewing window that enables visual liquid levels and separation process monitoring. Internally, its design incorporates weir for overflow. The multiphase fluid exits the test section and enters the first partition of the separator where the viewing window is located. Initial separation by gravity takes place in this section. The denser phase settles at the bottom while the less dense phase moves to the second section for further separation. A mixture of high-viscosity oil-water-sand may require a residence time of at least 18 – 24 hours for a near-complete separation to take place. After separation has taken place in the primary separator, oil (with possibly, little mixture of water) is pumped into the secondary separator where further separation takes place. The secondary separator is a modified Intermediate Bulk Container (IBC). On complete separation of the oil-water phase (after a residence time of about 6 hours), single phase oil is recovered and reused while wastewater from the (primary & secondary stage) separators and sand from the first stage separator are disposed of.

2.2.4 Instrumentation and Data Acquisition System

In the 1-inch horizontal and inclined facilities, two GE Druck static pressure transducers, PMP 1400 with pressure range 0 – 4 barg and accuracy 0.04% over the full scale is used to obtain the static pressure in the test sections. Both transducers are placed 2.17 m apart with the first of them positioned 60 pipe diameters from the last injection point, to ensure measurements are taken when flows are fully developed. A differential pressure transducer, Honeywell STD120, with minimum pressure drop measurement of 100 Pa and an accuracy of ±0.05% is used to measure the differential pressure. Temperature of the test fluids on the test section is measured by means of J-type thermal couples with an accuracy of ±0.1°C placed at different locations. Similar arrangement is used in the 3-inch test facility. For temperature regulation in the 1-inch horizontal and inclined test facilities, temperature (and hence viscosity) of mineral oil is regulated by a system consisting of a J-type thermocouple, copper coils (submerged in the oil tanks) and a Thermo Scientific (HAAKE Phoenix II) refrigerated bath circulator. Copper coils in the oil tank are connected to the circulator by running cold or hot glycol in the coils at specific time intervals. The temperature of oil in the tank is thus controlled by heat transfer. The

272 circulator's temperature ranges from 0 to +50 $°C$, with an accuracy of ± 0.01 $°C$. Similar
273 setup exists for temperature regulation of oil in the 3-inch facility. For repeatability and
274 reproducibility, selected test matrix (chosen in such a way that each test points are
275 represented) were repeated four times. Results showed good agreement for similar flow
276 parameters. This also agreed with uncertainty analysis carried out to estimate errors in
277 measurement. Please refer to Appendix A for information of how the uncertainty was
278 analysed.

279 Recordings of experimental test runs were done with two Sony Handycam HDR-
280 CX550VE, 12.0 Megapixels, Wide Angle 26.3 MM, Exmor R CMOS Sensor, 1080 50i
281 PAL Full HD, G Lens, focal length 3.8~38.0 mm with sampling frequency of 25 Hz. Both
282 cameras were placed 50 cm from the viewing sections in the side and bottom positions
283 to ensure flow features of sand particulates from those positions are clearly captured Two
284 lamps powered by four 40 W bulbs each were used to illuminate the test section, the lamp
285 were placed at 45 degrees inclination to the section to minimize reflections.

286 **2.3 Test procedure**

287 The procedure used to conduct the test is described. Mineral oil stored in the oil tank is
288 pumped through a recirculation loop between the oil tank and the test facility
289 bypass/injection section to ensure a uniform temperature distribution (and thus, liquid
290 viscosity). Set temperature on the chiller is used to regulate oil viscosity. Temperature at
291 the tank, the viscometer and operating temperature at the single-phase oil line just before
292 the injection point are used to validate the viscosity of the single-phase oil before it mixes
293 with water at the mixing section. In the main test section, transducers are used to log
294 temperature values. Analysis of the data shows that temperature at the main test section
295 are similar to temperature at the tank. The oil tank has submerged temperature controller
296 coils to ensure either heating or cooling of the contents in the tank. On the inception of
297 any experiments, data is first obtained for an empty test section and a single-phase filled
298 facility to ensure noise and zero errors in the devices are eliminated during data analysis.
299 During experiment, oil is first pumped into the main test line through a pipe that is in-line
300 with the main test section and at flowrates that corresponds to the predetermined oil
301 superficial velocity. The superficial velocity of oil is then kept constant throughout the
302 experimental run time. Slurry is introduced through a flexible pipe connected to the main
303 test section by a Tee-section.

304

305 **Table 2: Test matrix for oil-water-sand experiments**

Pipe ID (m)	Inclination	Vso (m/s)	Vss (m/s)	Sand concentration (vol/vol)	Viscosity (Pa.s)
0.0254	0°	0.10 – 0.20	0.1 – 1.4	0.010 – 0.100	3.5, 10.0
0.0254	30°	0.10 – 0.20	0.1 – 1.0	0.010	3.5

| 0.0764 | 0° | 0.10 – 0.20 | 0.2 – 1.0 | 0.010 – 0.050 | 3.5 |

306 For tests geared towards obtaining MTC, slurry superficial velocity starts from a high
307 superficial velocity and decreases gradually. If the effect of shutdown is to be investigated
308 or pickup velocity of sand particles, slurry velocity begins from its lowest and gradually
309 increases. For each test condition, the flow is allowed to run for 60s from which 30s worth
310 of data is logged at sampling frequency of 250 Hz. In order to ensure results
311 reproducibility, selected test conditions (40% of the test matrix for each experimental run)
312 across the different flow patterns are repeated three times, measurements are obtained
313 during each run and their results are compared to ensure consistency. Video recordings
314 and still photographs are recorded in both the side and bottom view of the test observation
315 section. Table 2 shows the test matrix used for the experimental investigations carried
316 out in this study for the three experimental test facilities.

317 **3 Results and Discussion**

318 **3.1 Flow Characterization**

319 Results and discussion for the flow patterns observed in test facilities with 1-inch, 1-inch
320 inclined and 3-inch pipe internal diameters are presented here. The section describes the
321 flow patterns with the aid of images and presents a flow pattern map to highlight the flow
322 condition in which each flow pattern was observed. The transitions from one pattern to
323 the other are highlighted in the map. Pipe diameter and inclination effects are also
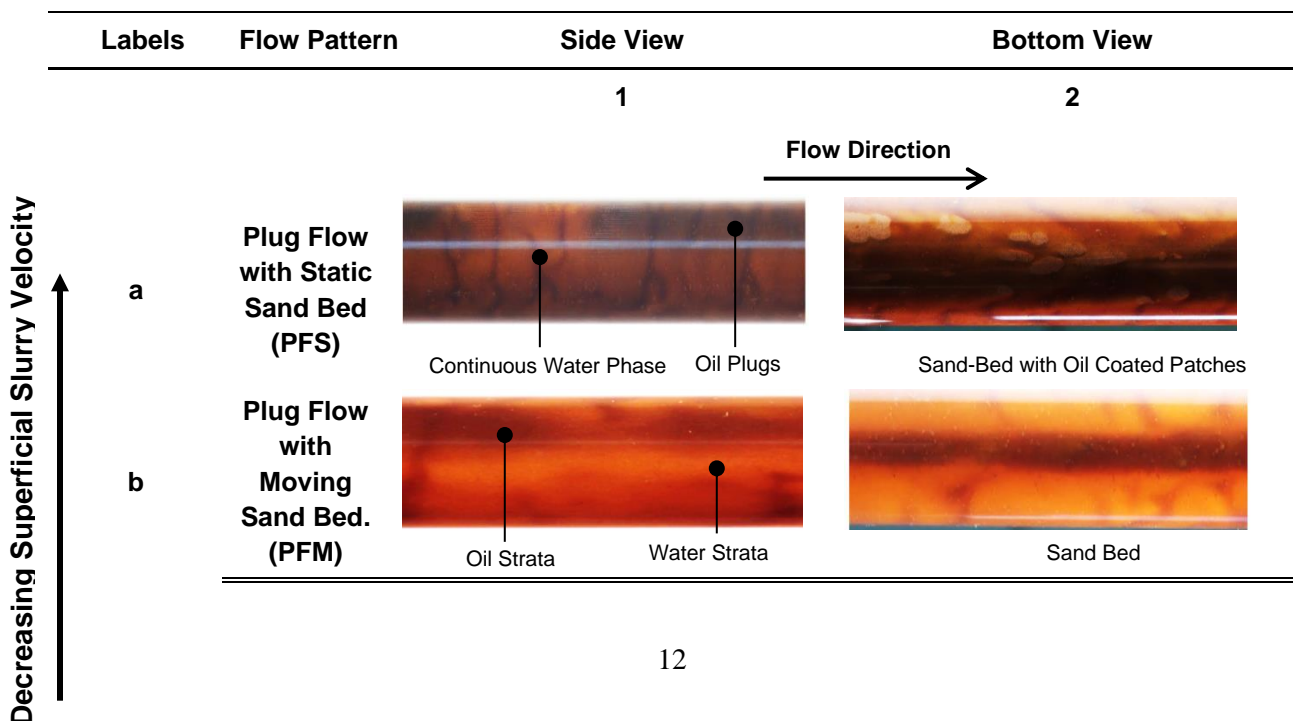324 discussed.

325 **3.1.1 Flow Pattern Maps**
326 Representative still images obtained from high definition cameras are presented in Figure
327 4. Images shown follows flow patterns observed with a gradual reduction in slurry velocity
328 from bottom to top. At the highest superficial slurry (water-sand) velocity and a fixed oil
329 superficial velocity, sand particles in the multiphase flow attains its highest momentum.
330 This momentum causes the sand particles in the pipelines to be dispersed in the flow in
331 a random and chaotic pattern. The degree of homogeneity of the particles in the liquid is
332 a function of the liquid velocity. This flow pattern observed is termed the *Dispersed Flow*
333 *(DF)* pattern is observed (Figure 4d)*.* DF is characterised by oil dispersion in a continuous
334 water phase (Figure 4d1 and 4d2). Fouling in the form of oil streaks on the pipe wall (as
335 a result of the high viscosity of oil) is observed in this regime with sand particles
336 homogeneously distributed.

337 When superficial slurry velocity is decreased, the very high momentum observed in the
338 DF is reduced, this allows some dispersed oil to form globules in water. These globules
339 (oil plugs) are observed to be flowing in a continuous water. Oil streaks on the pipe walls,
340 first noticed in the DF regime is observed to grow thicker due to a reduction in water cut
341 and sand concentration in the flow (decreased flow momentum ensures more oil is now

able to foul the pipe walls). Figure 4c2 shows a relatively lower homogenous distribution of sand particles relative to the *DF*. This is also attributable to the decrease in turbulent energies that enhanced sand particles dispersion. Further reduction in the slurry superficial velocity oil-coated sand particles are walls of the pipe. Figure 4c1 shows that oil plugs were predominantly near the top section of the pipe. This flow pattern was termed *Plug Flow (PF)*. Additional reduction of the slurry superficial velocity resulted in a flow pattern similar to *PF*. However, a moving/sliding sand bed was observed at the bottom of the pipe. The oil streaks on the walls of the pipe and the oil plugs increased in size relative to the *PF*. Flow patterns with these characteristic features were termed *Plug Flow with Moving Sand Bed (PFM)*. The onset of sand deposition at the bottom of the pipeline. This flow pattern was in the PFM. The mean mixture velocity of the flow at which the sand particles were observed to be sliding on the bottom (as shown in Figure 4b2) of the pipeline is the MTC . Further reduction in slurry superficial velocity resulted in a denser sand bed, elongated and thicker oil plugs. This is attributable to a reduction in flow turbulence which ensures more sand particles settle to the bottom of the pipe and the oil plugs agglomerate into thicker sizes as shown in Figure 4a2. In addition, gravity forces in flow are dominant at relative lower flow velocities leading to the settling of sand particles. Decreasing sand superficial velocity further, resulted in more sand particles settling at the sand bed as gravity forces dominance increases. Figure 4a2 shows that oil wetted sand particles were observed to agglomerate in patches within the sandbed. Some patches were observed to be moving at slow speed rlative to the mean speed of the sand bed. This flow pattern was termed the *Plug Flow with Static Sand Bed (PFS)*.

Flow pattern maps were constructed with the superficial oil and slurry velocities on the ordinate and abscissa respectively, as shown in Figure 5. From the plots shown, it is clearly seen that the transition from one flow pattern to the other depends on the oil superficial velocities, the sand concentration and the slurry velocity.
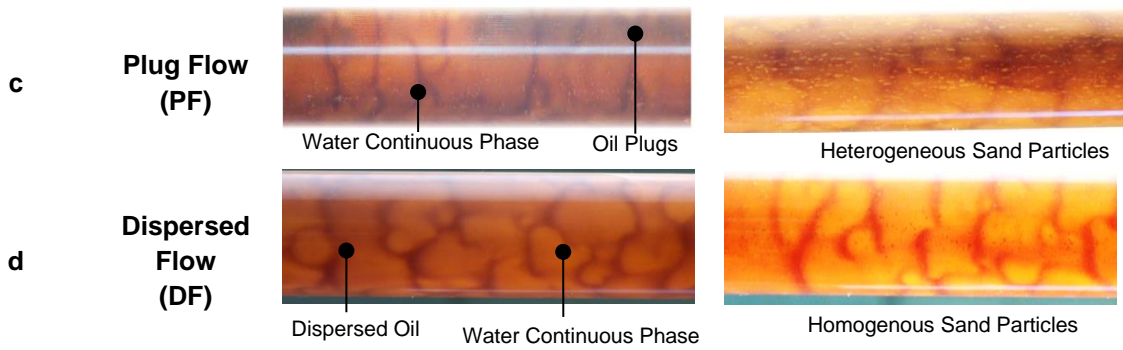
Labels	Flow Pattern	Side View	Bottom View
		1	2

Flow Direction →

| a | Plug Flow with Static Sand Bed (PFS) | Continuous Water Phase — Oil Plugs | Sand-Bed with Oil Coated Patches |
| b | Plug Flow with Moving Sand Bed. (PFM) | Oil Strata — Water Strata | Sand Bed |

Decreasing Superficial Slurry Velocity (↑)

c	**Plug Flow (PF)**	

Water Continuous Phase   Oil Plugs

Heterogeneous Sand Particles

d	**Dispersed Flow (DF)**	

Dispersed Oil   Water Continuous Phase

Homogenous Sand Particles

368 **Figure 4: Representative images of flow pattern in oil-water-sand flow**

369 Flow patterns earlier described transits from one type to the other based on this flow
370 conditions. As an example, for a fixed superficial oil velocity of 0.11 m/s at nominal oil
371 viscosity of 10.0 Pa.s and sand concentration of 10%, *DF* flow pattern is observed at the
372 highest slurry superficial velocity of 0.90 m/s. A reduction in this superficial velocity to
373 about 0.7 m/s sees the flow transit to *PF*. Subsequent reduction to lower slurry velocities
374 sees transition through the MTC to the *PFM* and the *PFS* flow patterns. For the 30°
375 inclined test section, a flow pattern map was similarly constructed and is shown in Figure
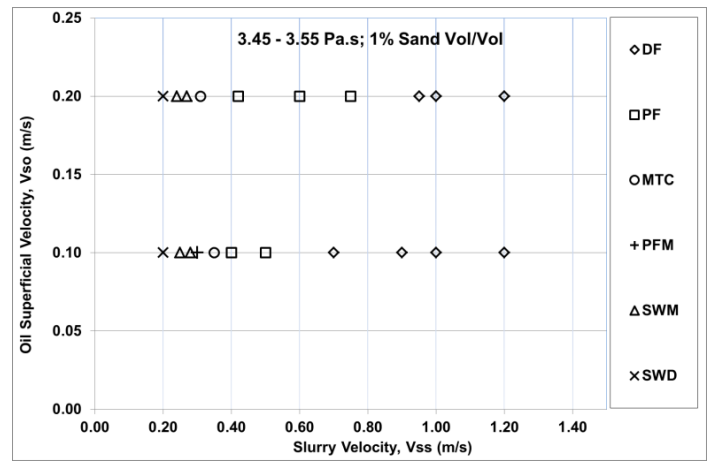376 5 (d). The different flow conditions at which each flow pattern exists are clearly shown in
377 the map.

(a)

(b)

13

(c)　　　　　　　　　　　　　　　　　　　(d)
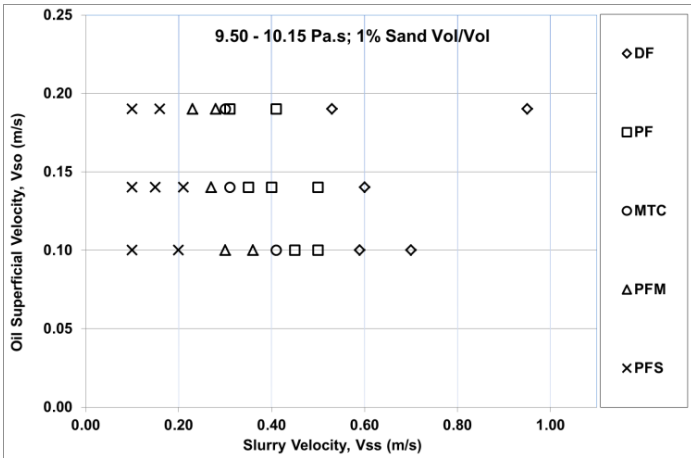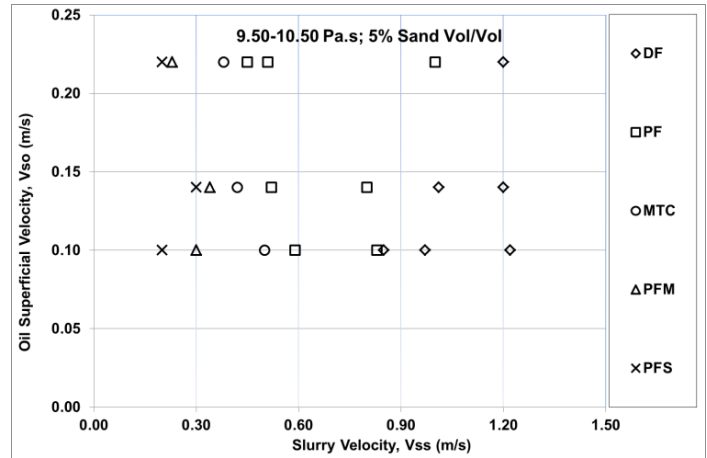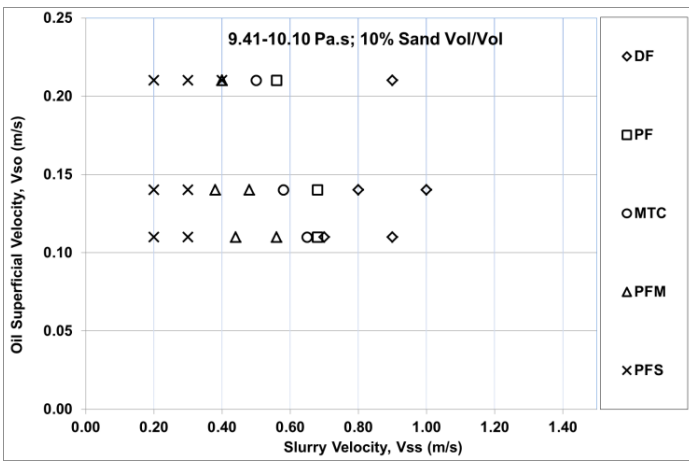
Figure 5: Flow pattern maps for oil-water-sand flow for sand concentrations of (a) 1% (b) 5% (c) 10% v/v at oil viscosity 10.0 Pa.s and (d) 1% v/v sand concentration at oil viscosity of 3.5 Pa.s.

Flow patterns observed in the 1-inch 30° upward inclined test section are shown in Figure 6 with increasing slurry superficial velocity from top bottom. For a constant superficial oil velocity and at the highest superficial slurry velocity tested in this investigation, *Dispersed Flow (DF)* is observed. Oil streaks and thus fouling on the pipe wall, hitherto observed in the horizontal test section, were considerably thinner and sometimes, non-existent in the inclined section. This may be attributable to the increased effect of gravity which enhances the draining speed of oil from the pipe walls. *Plug Flow (PF)* was observed on reducing the slurry velocity. Further reduction resulted in the *Plug Flow with Moving Sand Bed (PFM)* similar to the earlier description in the horizontal test section. At superficial velocities of slurry below *PFM*, a flow pattern in which oil, water and sand flowed in different strata was observed. The densest phase (sand) flowed at the bottom while the least dense phase (oil) flowed at the top. The interface between oil and water was wavy and irregular. The sand bed in this regime was transported along the pipeline at low velocities, it also thicker compared to *PFM*. This flow pattern was termed *Stratified Wavy Flow (SWM)*.
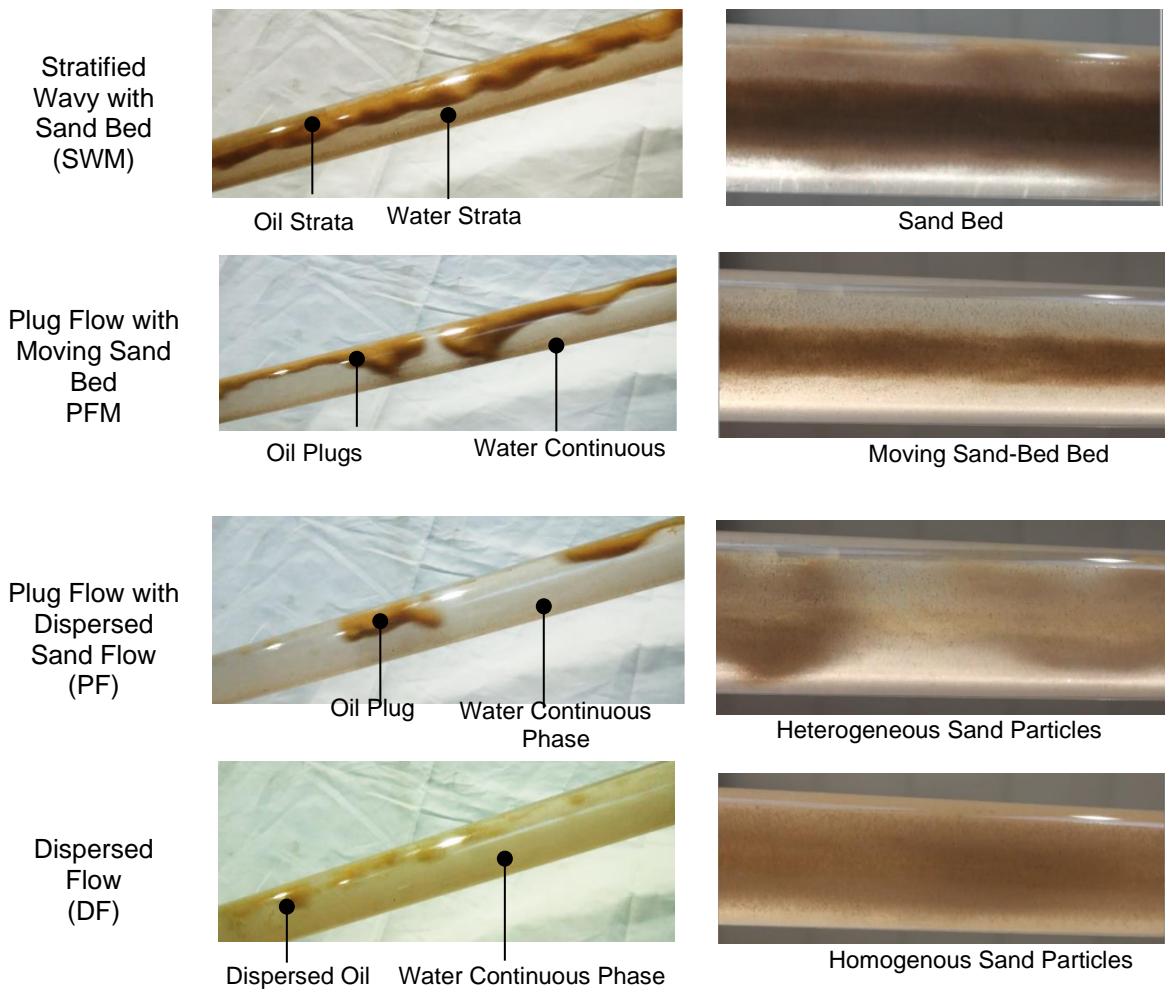

14
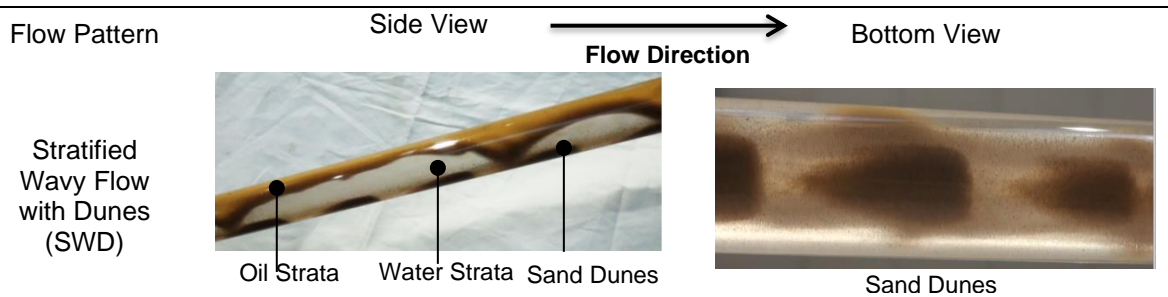
Figure 6: Flow Patterns in the 1 inch 30 degrees upward inclined pipe

A further decrease led to observations of flow pattern similar to the *SWM*, however, the moving sand bed were transformed to dunes, particles at the upper layer of the dunes were observed to be saltating into the sheds in front of its parent dune. The particles in the shed stayed in place until the slower moving dune travels the distance and reabsorbs the particle into its "cell". The wavy interface of the oil was observed to make infrequent contact with the sand particles at the dunes' topmost layer. This flow pattern was called *Stratified Wavy Flow with Dunes*, *SWD*. It is worth noting that *SWM* and *SWD* were not observed in the horizontal flow patterns at similar test conditions, their observation here can be explained by the increased effect of gravity in the flow due to test section inclination which favours flow stratification in high viscous oil-water flow.

3.2 Minimum Transport Condition (MTC)

The Minimum Transport Condition (MTC) is defined as: "*the slurry superficial velocity in which water wetted sand, deposits and forms a sliding/moving sand bed on the bottom of a horizontal or slightly inclined pipeline*". MTC of sand in oil-water multiphase flow test was determined through visual observations, video recordings and pressure gradient logs. Results obtained for MTC is discussed in the following subsections.

3.2.1 Effect of Oil Superficial Velocity on MTC

MTC results in the 1 inch horizontal test facility for nominal oil viscosity, 10.0 Pa.s and sand concentrations of 1, 5 & 10% volume/volume is presented in Figure 7. For sand concentration of 1% vol./vol. and nominal oil viscosity of 10 Pa.s, an increase in oil superficial velocity from 0.10 m/s to 0.14 m/s results in MTC reduction from 0.41 m/s to 0.26 m/s.
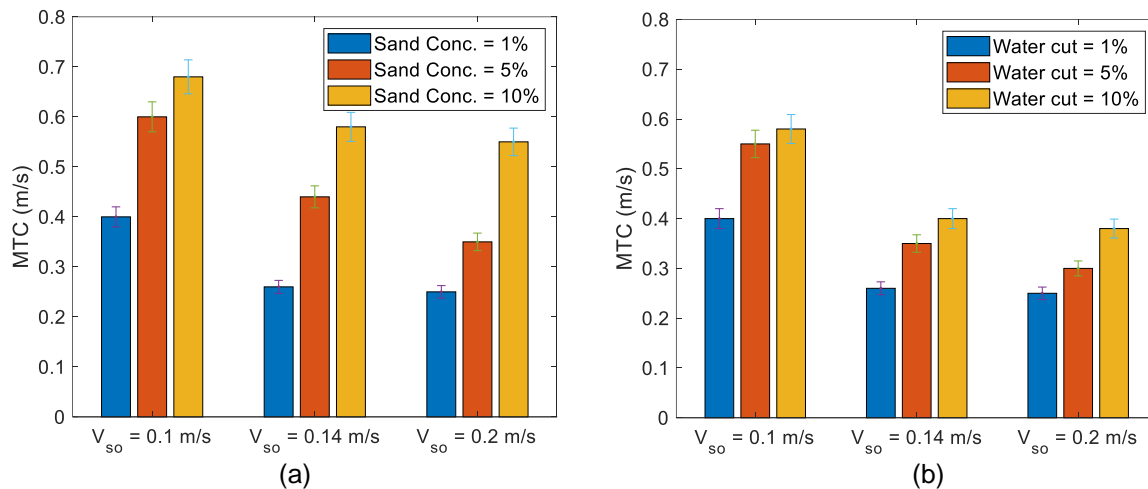

Figure 7: MTC as a function of oil superficial velocity, (a) sand concentration and (b) water cut at oil viscosity of 10.0 Pa.s

Further increase in oil superficial velocity from 0.14 m/s to 0.20 m/s marginally decreased the MTC to 0.25 m/s. The same trend is observed for sand volume fractions of 5 and 10%. This decrease in MTC with increase in oil superficial velocity indicates that an increased in oil content in the pipeline have the effect of increasing sand transportation capabilities of sand. Overall, an increased mixture velocity (sum of slurry and oil superficial velocities) will ensure increased turbulence thus ensuring sand particles remain suspended in flow at relatively lower MTC.

3.2.2 Effect of Sand Concentration on MTC

Figure 7 a shows that an increase in sand concentration have the effect of increasing the MTC for all the oil superficial velocities investigated. Gravity forces that acts to force sand particles to settle on the pipe's bottom is a function of gravitational acceleration and mass of the sand. Increasing the sand concentration will increase the mass of sand in the pipeline and hence, gravity forces. This implies that the gravity forces dominate over a relatively larger mixture velocity thus requiring a relatively larger superficial velocity for the onset of sand particles settling in the pipe's bottom. This characteristic behaviour, therefore, results in a higher MTC value. Higher lift forces are also required to keep sand particles in suspension. This trend of MTC increase with an increase in sand concentration was also observed for the low viscosity water-sand flow investigated by Archibong-Eso et al. (2019), Fajemidupe et al. (2019), Archibong-Eso (2015), and Yan (2010).

16

3.2.3 Effect of Water Cut on MTC

Figure 7 b shows water cut ($V_{ss}/(V_{ss} + V_{so})$) as a function of both the oil superficial velocity and the sand concentration. It is pertinent to note that in this study, a modified water cut equation was used by substituting the water superficial velocity with slurry superficial velocity. For the three-sand concentrations investigated in this study, water cut values at the MTC reduced with increase in oil superficial velocity. This follows a similar explanation made earlier; increased oil superficial velocity increases the turbulence in flow hence allowing suspension of particles at lower water cut. Practically, this implies that for fields with high oil content, the water cut required to transport sand particles will be lower compared to a similar field with low oil content.

3.2.4 Viscosity effects on MTC

Experimental investigations conducted with oil viscosity of 3.5 Pa.s and 10.0 Pa.s in the 1-inch horizontal flow loop are used to discuss the effect of viscosity on MTC for sand. Results shown in Table 3

Table 3 indicates that the MTC for three-phase oil-water-sand flow increased with increase in MTC for both sand concentrations used in this section of the study.

Table 3: Viscosity effect on MTC

Vso (m/s)	Oil Viscosity (Pa.s)	Sand Concentration (%)	MTC (m/s)
0.10	3.50	1.00	0.32
0.10	3.50	5.00	0.36
0.10	10.00	1.00	0.41
0.10	10.00	5.00	0.60
0.10	10.00	10.00	0.66

While an increase of about 28% was observed at 1% sand concentration when oil viscosity increased from 3.5 Pa.s to 10.0 Pa.s, a similar increase in oil viscosity at 5% sand concentration yielded a 67% increase in MTC value. Kinetic turbulence is essential in ensuring sand particles are suspended during the three-phase flow, an increase in oil viscosity reduces the turbulence thus ensuring that particles require a much higher flow velocity to produce significant inertia forces capable of overcoming the viscous forces.

3.2.5 Pipe diameter effects on MTC

The 3-inch horizontal test facility was used to investigate the effect of scaling up the internal pipe diameter on MTC. Sand concentration studied was 1 and 5% at oil viscosity of 3.5 Pa.s and oil superficial velocity of 0.10 – 0.20 m/s. Table 4 presents the result obtained from both horizontal facilities. Result indicates that MTC increased with increase in pipe diameter at the same oil superficial velocity. Comparatively, MTC increased from 0.57 m/s at sand concentration of 1% and oil superficial velocity of 0.10 m/s in the 1-inch

472 pipe to about 0.72 m/s in the 3-inch pipe at similar flow conditions. Similar trend is
473 observed for the 5% sand concentration. This may be attributed to the decrease in the
474 flow turbulence for similar flow conditions. As pipe diameter increases and thus the
475 effective flow area, Reynolds Number, a major pointer to the turbulence in flow (which
476 acts to keep sand particle suspended rather than depositing on the pipe's bottom)
477 decreases hence requiring higher velocities to keep the same sand concentration
478 suspended in flow.

479 **Table 4: Oil-Water-Sand MTC in 1 and 3-inch ID test facilities**

| Oil Superficial Velocity (m/s)	Sand concentration (%)	Pipe Diameter (m)	Oil Viscosity (Pa.s)	MTC (m/s)
0.10	1.00	0.0254	3.50	0.32
0.10	1.00	0.0764	3.50	0.54
0.19	1.00	0.0254	3.50	0.25
0.20	1.00	0.0764	3.50	0.76
0.10	5.00	0.0254	3.50	0.36
0.11	5.00	0.0764	3.50	0.88

480 ### 3.2.6 Inclination Effects on MTC
481 Results obtained from the 1-inch 30° inclined test section were used to compare with the
482 1-inch horizontal test section for the oil-water-test as shown in Table 5. Results indicate
483 that within the test conditions of the experiments, MTC is only slightly affected by the
484 inclination angle. MTC at 30° test section was similar to that of the horizontal with only
485 slight changes observed. Generally, it was observed that a 30° upward inclination had
486 negligible effect on MTC when compared to the horizontal test for oil-water-sand flows.
487 Results presented are for nominal oil viscosity of 3.5 Pa.s.

488 **Table 5: MTC for oil-water-sand test in horizontal and inclined test facilities (Nominal oil viscosity,**
489 **3.5 Pa.s)**

Sand concentration (%)	Pipe Diameter (m)	Inclination (°)	Oil Superficial Velocity (m/s)	MTC (m/s)
1.00	0.0254	0	0.10	0.42
1.00	0.0254	30	0.10	0.41
1.00	0.0254	0	0.14	0.44
1.00	0.0254	30	0.15	0.46
5.00	0.0254	0	0.20	0.54
5.00	0.0254	30	0.20	0.55

490
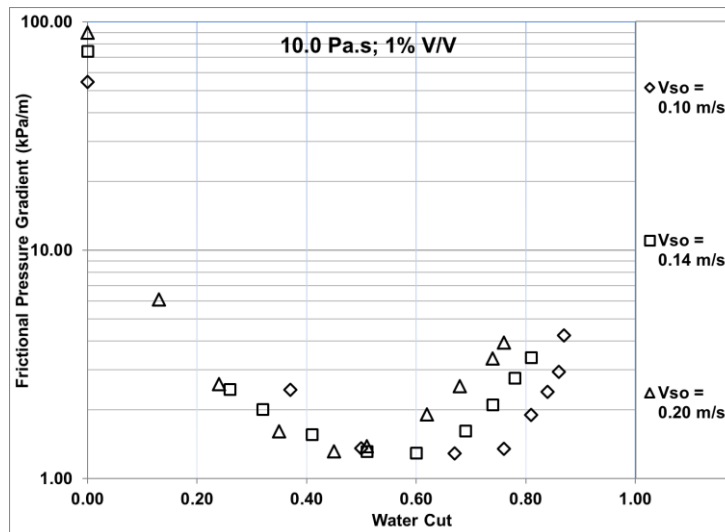
Figure 8: Pressure gradient as a function of water cut (sand concentration, 1% v/v) – 30º inclined pipeline.

3.3 Pressure Gradient Analysis

3.3.1 Effect of Water Cut on Pressure Gradient

Figure 8 shows plots of pressure gradient as a function of water cut for representative flow conditions in the study. It is observed that initial increase in water cut decreases the pressure gradient due to the reduction of the effective viscosity in the flow until a minimum is reached. Further increase is observed to result in a corresponding increase in pressure gradient; this is because the increased water cut has relatively little effect on viscosity reduction compared to the increased flow velocity, which aids pressure increase. Additionally, some of the dispersed oil and oil plugs are carried back to the walls of the pipe resulting in increased shear. This behaviour is particularly similar to the water-oil flow.

3.3.2 Effect of Oil Input Content on Pressure Gradient

The effect of increasing oil input content (oil superficial velocity) on pressure gradient is shown in Figure 9 below where pressure gradient as a function oil superficial velocity of 0.10, 0.14 and 0.20 m/s are presented. The plot shows a general increase in pressure gradient with increase in oil superficial velocities. This is attributed to the increase oil content in the line. An increase in oil content increases the shear on the pipe wall and thus the pressure gradient as earlier explained in the oil-water-sand 1-inch horizontal test. Notably, below a slurry velocity of about 0.2 m/s (where the flow is largely unassisted by water), the effect of increasing the oil content in the pipe is not distinct. Further investigations may be necessary to determine the flow characteristic behaviour.
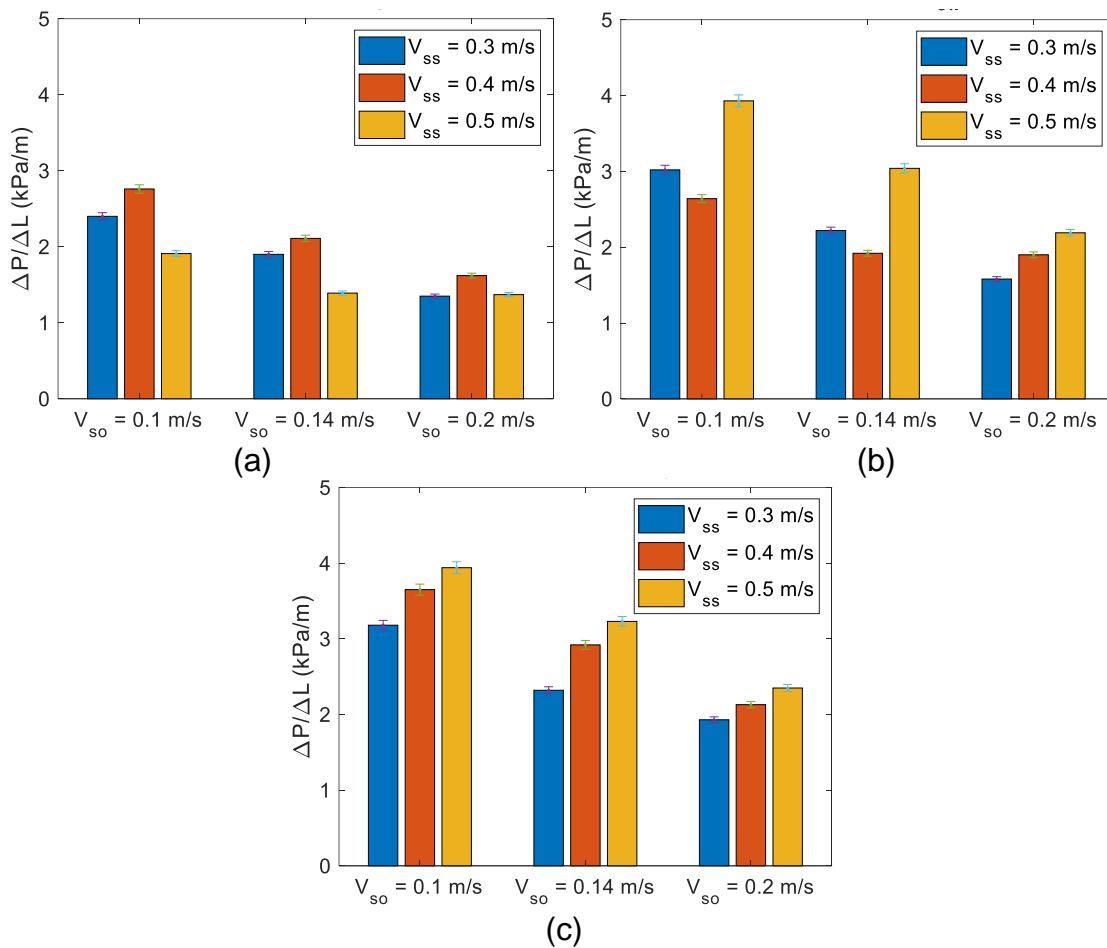
Figure 9: Pressure gradient as a function of oil and sand superficial velocities at sand concentration of (a) 1% (b) 5% and (c) 10% v/v and oil viscosity of 10 Pa.s.

A further explanation on the effect of oil input on pressure gradient can be made using the superficial oil velocity. For all the conditions depicted in Figure 9, the pressure gradient progressively declines with a reduction in slurry velocity. However, the magnitude of the pressure gradients increases with increasing oil viscosity due to the combined effect with sand concentration. For example, at Vso of 0.1 m/s, the pressure gradient is seen to increase from about 2 kPa/m to just below 3 kPa/m. Furthermore, it can be seen in Figure 9 c that the pressure gradient experiences a sharp increase as Vso goes from 0.14 to 0.2 m/s. From the Hagen-Poiseuille pressure gradient model, it is observed that pressure gradient is an inverse function of pipe flow area (diameter) thus explaining the observed phenomenon. Several authors in literature have stated that MTC occurs at the minimum pressure gradient in liquid-solid studies, this was not necessarily the case in the present study. Howbeit, the minimum pressure gradient reduction occurred close to the MTC and the disparity in conclusion may be a result of the differences in MTC definition, uncertainty in measurements and/or the subjectivity involved in MTC definition.

In comparison to the pressure gradient data of Mckibben et al. (2013) in their 4-inch pipe, the range of pressure gradients we obtained in the 3-inch pipe were similar in magnitude as theirs. However, the trend with mixture velocity (V_m) showed that the current data had

534 a gentler rising slope (especially at the 1% sand concentration case) as compared to
535 Mckibben's trend which had a linear and quasi-quadratic trend for their various water cut
536 and single phase conditions. These were given in Figure 4 of their article. The oils used
537 in their experiments had a range from 0.2–3.7 Pa.s and then a big jump to 31.4 Pa.s. As
538 such, their friction factor correlation's applicable range is affected by the missing
539 viscosities between 3.7 and 31.4 Pa.s. It is reiterated here that the current data were
540 obtained with oils of 3.5 – 10 Pa.s which may considered a more stable range. Secondly,
541 it is noted that our flow regimes were varied (oil plugs to dispersed oil with sand beds) as
542 against their co-annular regime. It is hence imperative to adjust the friction factor
543 correlation to be more applicable to the conditions of the current experiments. We report
544 the correlation procedure in subsequent sections.

545 3.3.3 Effect of Sand Concentration on Pressure Gradient

546 Table 6 below shows the pressure gradient at MTC for different sand concentration at the
547 same superficial oil velocity. Results shown indicates that the pressure gradient increases
548 with increase in sand concentration, this is expected as the increased sand concentration
549 in the flow line decreases the effective flow area of the mixture thereby increasing the
550 pressure gradient.

551 **Table 6: Sand concentration effect on pressure gradient**

Sand concentration v/v (%)	Vso (m/s)	Oil Viscosity (Pa.s)	MTC (m/s)	Pressure Gradient (kPa/m)
1	0.10	10.0	0.51	1.90
5	0.10	10.0	0.60	3.02
10	0.10	10.0	0.66	3.18

552
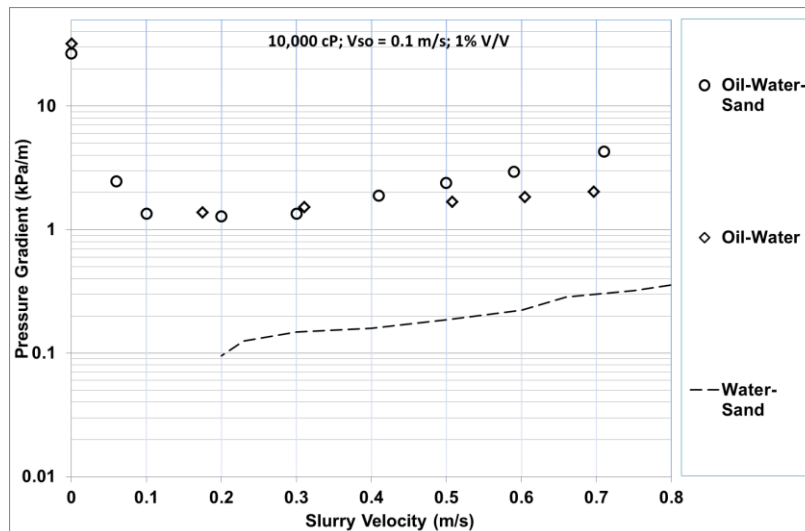
553 **Figure 10: Pressure gradient as a function of slurry velocity (or water superficial velocity) in a**
554 **variety of multiphase flow**

21

3.3.4 Water-Sand, Oil-Water & Oil-Water-Sand Pressure Gradient

Comparison of pressure gradient obtained in water-sand, oil-water and oil-water-sand flow against slurry velocity (or water superficial velocity, as in the case of oil-water flow) is presented in Figure 10. Comparatively, at similar flow conditions, oil-water pressure gradient is lower than the pressure gradient logged for oil-water-sand; the presence of sand in the latter may be responsible for this observation. Sand in flow acts to reduce the effective flow area of the pipe thus increasing the pressure gradient. A further comparison with the water-sand test shows clearly the influence of oil and sand presence in flow. In comparison between the water-sand, oil-water and oil-water-sand flow, it is observed that the water-sand flow pressure gradient was the lowest by several order of magnitudes due to the absence of oil in flow. The presence of oil in flow results in increase shear and fouling on the pipe wall, hence increasing the pressure gradient.

3.4 Correlation for MTC in oil-water-sand pipe flow

Based on the experimental data collected that have been collected, it is imperative to correlate the onset of sand transport in three-phase oil–water–sand flow. Since it was shown that MTC varies as a function of the inlet oil and water conditions as well as the sand slurry flow conditions, these quantities will be used for correlation in dimensionless form. The correlation method is based on the method of McKibben et al. and can be considered an improvement of their model. A similar method have been adopted by(Aliyu, 2015; Aliyu et al., 2015) The MTC which gives the onset of particle deposition in the pipeline, is defined as the condition whereby the friction velocity is greater than the particles' terminal settling velocity i.e. when $V^* > V_\infty$. The settling velocity is defined as

$V_\infty = \sqrt{1.33 \, gD(\rho_S - \rho_f)/C_D\rho_f}$; where ρ_f and C_D are the solid carrier fluid (water) density and the drag coefficient of the solids respectively. Other parameters are as previously defined. In fact, Mckibben et al. found that with oils of up to 31.4 Pa.s, the relationship between the friction velocity and the particle terminal settling velocity at MTC is as follows.

$$V^* = 9V_\infty \tag{1}$$

meaning that the minimum transport condition or velocity is:

$$V_{MTC} = \frac{9V_\infty}{\sqrt{f_m/2}} \tag{2}$$

since the friction velocity and the terminal settling velocity are related by:

$$V^* = V_{MTC}\sqrt{\frac{f_m}{2}} \tag{3}$$

where f_m is the three-phase mixture friction factor which McKibben et al. (2013) found the following relation to fit their experimental data:

22

$$f_m = 15 \cdot Fr^{-0.5} f_w^{1.3} f_o^{0.32} C_w^{-1.2} \tag{4}$$

585   where Fr, is the mixture Froude number, f_w is the mixture friction factor for the water
586   phase, C_w is the water cut (water fraction), and f_o is the oil friction factor. They are r
587   defined as follows:

$$Fr = \frac{V_M}{\sqrt{gD}} > 0.35; \qquad f_w = \frac{1}{\sqrt{16 \log \sqrt{5.7/\rho_m V_M^2 D}}}; \tag{5}$$

$$f_o = \frac{16}{Re} \qquad Re = \rho_o V_m D / \mu_w$$

588   For the current study, as the viscosity range is lower than that used by McKibben and co-
589   workers, we therefore correlated the mixture friction factor using the measurements
590   obtained the current study in addition to those of McKibben's using non-linear least
591   squares fitting. For simplicity, the same dimensionless parameters used by McKibben et
592   al. (2013) were selected since they carried out an extensive dimensional analysis. We
593   therefore express f_m as a power law function of Fr, f_w, f_o, and C_w as follows:

$$f_m = A \cdot Fr^b f_w^c f_o^d C_w^e \tag{6}$$

594   where the coefficient A and indices b-e are regression constants to be determined by
595   fitting Equation 6 to the horizontal experimental data for the two pipe sizes in this study,
596   using the least squares method expressed as a minimisation problem as follows:

$$min \sum_{i=1}^{N} \left[(f_m)_{exp,i} - (A \cdot Fr^b f_w^c f_o^d C_w^e)_{pred,i} \right]^2 \tag{7}$$

597   where N is the number of experimental data points, the subscripts "*pred*" and "*exp*" denote
598   predicted and experimental respectively. Equation 7 was solved iteratively to determine
599   the values of A–e using the Generalised Reduced Gradient method. Initial values of A–e
600   were chosen and constrained to be realistic. Hence, the new three-phase friction factor
601   correlation, which covers a wider range of experimental conditions and oil viscosity, is
602   given as:

$$f_m = 20 \cdot Fr^{-0.5} f_w^{1.2} f_o^{0.4} C_w^{-0.32} \tag{8}$$

603   It will be shown in Figure 11 that the MTC predicted using the new correlation is a marked
604   improvement over that using Equation (4). In addition to the new mixture friction factor
605   correlation (Equation 6), calculation methods for other key quantities in the MTC
606   correlation were employed that consider the mechanisms at play. For example, for
607   calculating the terminal velocity, the Burddyck model was used. It was developed for the
608   transition zone ($0.1 < d_p < 0.1 \ mm$) and clearly defines the characteristic drag coefficient
609   of the particles:

$$V_\infty = \frac{8.8}{d_p}\left[\sqrt{1 + 95\frac{S_s - S_f}{S_f}d_p^3} - 1\right] \tag{9}$$

610 where d_p, S_s and S_f are defined as the particle diameter, specific density of solids relative
611 to water, and the specific density of carrier fluids relative to water. Secondly, an effective
612 diameter, D_H is used for implementation to ensure the flow area takes the presence of
613 sand particles into account. This is achieved by estimating a sand holdup, H_s and hence
614 the effective diameter for the flow area:

$$H_s = \frac{C_v V_{ss}}{V_m} \tag{10}$$

$$D_H = D(1 - H_s) \tag{11}$$

615 where C_v and D are the sand concentration and the pipe internal diameter respectively.
616 To account for the sand concentration, the gravity effect is associated with the sand
617 concentration thus: $g(s - 1)(1 - C_v)$. This is consistent with the fact that the gravity force
618 in flow is associated to the weight of sand and thus its concentration in the flow line. It is
619 worth noting that at lower sand concentration this may be negligible. However, as sand
620 concentration increases it becomes increasingly important and will lead to errors in the
621 model if not considered. Therefore, a modified Froude number is used:

$$Fr = \frac{V_m}{\sqrt{gD_H(s - 1)(1 - C_v)}} \tag{12}$$

622 Figure 11 shows that the McKibben et al. (2013)'s model over estimates the MTC by up
623 to 50%, this error in prediction may be attributed to the fact that the model was developed
624 on the basis of significantly different flow conditions (e.g. pipeline used in their study had
625 internal diameters of 4 and 6-in) and fluids of a higher viscosity range than those used in
626 the current experiments. On the other hand, the MTC prediction based on the modified
627 friction factor which was derived by combining the current experimental data and those
628 of McKibben et al.'s shows markedly improved predictions which are predominantly within
629 a $\pm20\%$ error band.
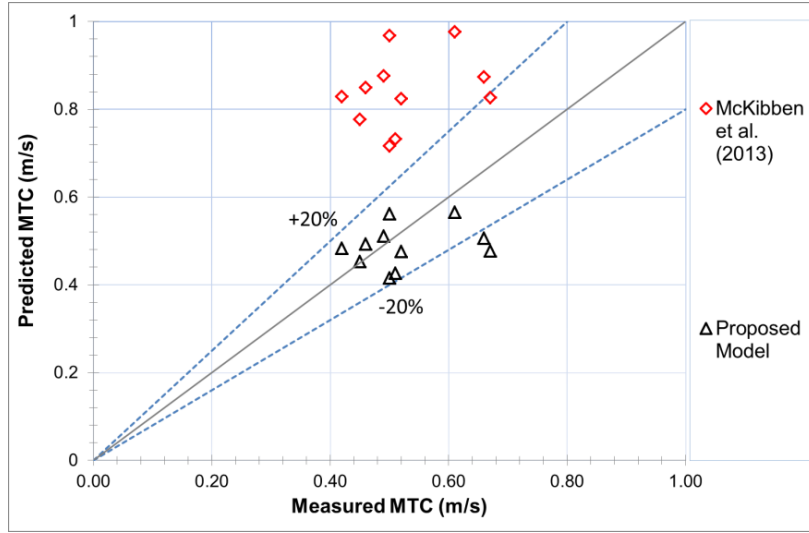
Figure 11: Comparison of McKibben et al. (2013) Model with the proposed modified model

Table 7 shows the statistical performance evaluation of the new model and that of Mckibben's. The evaluation indicates that the proposed model outperforms Mckibben's MTC model for all the statistical errors investigated. The statistical parameters E_1–E_4 are defined for each data point i as follows. E_1 is the average relative error:

$$E_1 = \frac{1}{N}\sum_{i=1}^{N}(y_{predicted} - y_{measured})_i \tag{13}$$

he absolute of average relative error is given as:

$$E_2 = \frac{1}{N}\sum_{i=1}^{N}\left|(y_{predicted} - y_{measured})_i\right| \tag{14}$$

While standard deviation about the relative error is given by:

$$E_3 = \sqrt{\frac{\sum_{i=1}^{N}(y_i - Y_1)^2}{N-1}} \tag{15}$$

The average actual error

$$E_4 = \sum_{i=1}^{N}\left(y_{predicted} - y_{measured}\right)_i^2 \tag{16}$$

The mean error, E_1, the mean absolute error, E_2, standard deviation, E_3 of the errors and the sum square of errors, E_4 of the proposed model were -0.03, 0.17, 0.19 and 0.42 respectively relative to McKibben's model of 0.63, 0.63, 0.24 and 5.08 respectively. Caution is advised in using the correlation outside the range of experimental data used in its development. Nevertheless, the correlation provides a useful tool in obtaining

644 improved predictions of sand MTC in three-phase oil–water–sand flows involving highly-
645 viscous oils.

646 Table 7: Statistical evaluation of proposed model with the McKibben et al. (2013) model

Correlation	E1	E2	E3	E4
McKibben et al. (2013)	0.63	0.63	0.24	5.08
Proposed	-0.03	0.17	0.19	0.42

647

4 Conclusions

649 In this study, the transport of high viscous oil-water-sand has been experimentally
650 investigated in the 1 & 3-inch horizontal and 1-inch 30˚ upward inclined test facilities. The
651 study involved flow pattern identification, pressure gradient analysis and MTC prediction.

652 The main findings in the study are as follows:

653 In the horizontal multiphase oil-water-sand test, new flow patterns namely: Dispersed
654 Flow *(DF)*, Plug Flow *(PF)*, Plug Flow with Moving Sand Bed *(PFM)* and Plug Flow with
655 Stationary Sand Bed *(PFS)* were reported in the horizontal pipe.

656 For the inclined flow, similar flow patterns were observed with two additional flow patterns;
657 the Stratified Wavy Flow with Moving Sand Bed *(SWM)* and Stratified Wavy Flow with
658 Dunes, *(SWD).*

659 Pressure gradient were generally observed to decrease initially with decrease in
660 superficial slurry velocity (and hence water cut) before reaching a minimum. Further
661 reduction in the slurry velocity beyond this minimum results in an increase in pressure
662 gradient. Pressure gradient in the oil-water-sand test was much higher than the water-
663 sand test and higher when compared to the oil-water test for similar flow conditions.

664 The MTC in oil-water-sand test were observed to be largely the same for the 1-inch 30°
665 upward inclined and the 1-inch horizontal test section while that of the 3-inch horizontal
666 test section was considerably higher. A new empirical model has been proposed and
667 shown to outperform other sand–oil–water models including that of McKibben et al.
668 (2013).

Acknowledgement

677 **References**

678 Archibong-Eso A., Aliyu, A.M., Yan, W., Koneke, N.E., Baba, Y.D., Fajemidupe, O.T., Yeung, H.
679   (2020). Experimental Study on Sand Transport Characteristics in Horizontal and Inclined Two-
680   Phase Solid-Liquid Pipe Flow. Journal of Pipeline Systems Engineering and Practice. Vol. 11.
681   No. 1. 4019050

682 Archibong-Eso Archibong, Y. Zhao, H. Yeung, (2014) Comparison of electrical capacitance
683   tomography & gamma densitometer measurement in viscous oil-gas flows. AIP Conference
684   Proceedings 1592.

685 Archibong-Eso Archibong (2015) Viscous Multiphase Flow Characteristics in Pipelines (PhD
686   Thesis) Cranfield University, United Kingdom.

687 Archibong-Eso Archibong-Eso, Y. Baba, A. Aliyu, Y. Zhao, W. Yan, H. Yeung (2018) On slug
688   frequency in concurrent high viscosity liquid and gas flow, Journal of Petroleum Science and
689   Engineering, Volume 163, Pages 600-610,

690 Al-Safran, E Al-Qenae, K. (2018). A Study of Flow-Pattern Transitions in High-Viscosity Oil-and-Gas Two-
691   Phase Flow in Horizontal Pipes. Society of Petroleum Engineers. doi:10.2118/187939-PA

692 Aliyu, A.M., Baba, Y.D., Lao, L., Yeung, H. and Kim, K.C. (2017) 'Interfacial friction in upward
693   annular gas–liquid two-phase flow in pipes', *Experimental Thermal and Fluid Science*, 84, pp.
694   90–109. Available at: 10.1016/j.expthermflusci.2017.02.006 (Accessed: 21 February 2017).

695 Aliyu, A.M., Lao, L. and Yeung, H. (2015) 'A New Empirical Correlation for Entrained Droplet
696   Fraction Prediction in Co- current Gas – Liquid Annular Two-phase Flow in Large Diameter
697   Pipes 1 Introduction', *APCChE 2015 Congress incorporating Chemeca 2015*, (3131582), pp.
698   90–101.

699 Baba, Y.D., Aliyu, A.M., Archibong, A.-E., Almabrok, A.A. and Igbafe, A.I. (2017a) 'Study of high
700   viscous multiphase phase flow in a horizontal pipe', *Heat and Mass Transfer/Waerme- und
701   Stoffuebertragung*, 54(3), pp. 651–669.

702 Baba, Y.D., Aliyu, A.M., Archibong, A.E., Abdulkadir, M., Lao, L. and Yeung, H. (2018) 'Slug length
703   for high viscosity oil-gas flow in horizontal pipes: Experiments and prediction', *Journal of
704   Petroleum Science and Engineering*, 165(February) Elsevier Ltd, pp. 397–411.

705 Baba, Y.D., Archibong, A.E., Aliyu, A.M. and Ameen, A.I. (2017b) 'Slug frequency in high viscosity
706   oil-gas two-phase fl ow : Experiment and prediction', *Flow Measurement and Instrumentation*,
707   54(December 2016) Elsevier, pp. 109–123.

708 British Petroleum Company (2019). BP Statistical Review of World Energy. London: British
709 Petroleum Co.

710 Chen, Y., Sun, X., Yan, T., Yao, D., Duan, R. (2020). Experimental study on micron-sized sand
711 particles transport in the water flow path of hydrates production wellbore. Journal of Natural
712 Gas Science and Engineering. Vol. 73. 103088

713 Crowe, T. C., (2005),"*Multiphase Flow Handbook".1st edition*.CRS Press, USA.

714 Fajemidupe, O.T., Aliyu, A.M., Baba, Y.D. Archibong-Eso, A., Okeke, N.E., Ehinmowo, A.B.,
715 Yeung, H. (2019a). Minimum Sand Transport Conditions in Gas-Solid-Liquid Three-Phase
716 Stratified Flow in Horizontal Pipelines. SPE Nigeria Annual International Conference and
717 Exhibition. 2019

718 Fajemidupe, O.T., Aliyu, A.M., Baba, Y.D., Archibong-Eso, A., Yeung, H. (2019b). Sand minimum
719 transport conditions in gas–solid–liquid three-phase stratified flow in a horizontal pipe at low
720 particle concentrations. Chemical Engineering Research and Design. Vol. 143. Pages 114 –
721 126.

722 Gillies, R., McKibben, M. and Shook, C. (1995), "Oil, Water and Sand Flow Experiments in a
723 Model Horizontal Well", Journal of Canadian Petroleum Technology, vol. 34, no. 9.

724 Hamidreza Karami, Carlos F. Torres, Eduardo Pereyra, and Cem Sarica (2016) Experimental
725 Investigation of Three-Phase Low-Liquid-Loading Flow, SPE Annual Technical Conference
726 and Exhibition, Houston, USA.

727 McKibben, M., Sanders, S., Gillies, R. (2013). A New Method for Predicting Friction Losses and
728 Solids Deposition during Water-Assisted Pipeline Transport of Heavy Oils and Co-Produced
729 Sand. Society of Petroleum Engineers. June 11. doi:10.2118/165480-MS

730 Matthew J. S. King, C. Paul Fairhurst, Trevor J. Hill (2001), Solids Transport in Multiphase
731 Flows—Application to High-Viscosity Systems, J. Energy Resour. Technol. Sep 2001, 123(3):
732 200-204.

733 Okeke, N.E., Adeyemi, O., Archibong-Eso, A., Baba, Y.D., Aliyu, A.M., Aluyor, E.O., Yeung, H.
734 (2019). Experimental Study on the Effect of Undulating Pipeline on Sand Transport in
735 Multiphase Flow. SPE Nigeria Annual International Conference and Exhibition.

736 Leporini, M., Marchetti, B., Corvaro, F., Giovine, G., Polonara, F., Terenzi, A. (2019) Sand
737 transport in multiphase flow mixtures in a horizontal pipeline: An experimental investigation.
738 Petroleum. Vol. 5. No. 1. Pages 161-170.

739 Turian, R., Hsu, F., Ma T. (1987), Estimation of the critical velocity in pipeline flow of slurries,
740 Powder Technology, Volume 51, Issue 1, 1987, Pages 35-47.

741 Wagg B. T, Fang, Y. and Birkett, D. (2009). CHOPS without Sand. Journal of Canadian Petroleum
742   Technology. Vol. 43 Issue 03. DOI: http://dx.doi.org/10.2118/72060-PA

743 Yang, Y.; Peng, H.; Wen, C. (2019). Sand Transport and Deposition Behaviour in Subsea
744   Pipelines for Flow Assurance. Energies. Vol. 12. 4070

745 Yan, W. (2010) Sand transport in multiphase pipelines, PhD thesis. Cranfield University, UK.

746 Zhao, Y.; Yeung, H.; Zorgani, E.E.; Archibong, A.E (2013) High viscosity effects on characteristics
747   of oil and gas two-phase flow in horizontal pipes Chem. Eng. Sci., 95, pp. 343-352

748

A.1 Estimating Uncertainties

750 In this research, work, experimental uncertainties were determined using a stepwise
751 procedure similar to (Archibong 2015) and it is explained below:

752 1. If an experimentally measured output, y is a function of inputs $x_1, x_2, x_3 \ldots x_n$ then:

$$y = f(x_1, x_2, x_n \ldots x_n) \tag{A-1}$$

753 2. Estimate uncertainty of x_i

754 $\qquad u(x_i) -$ uncertainty in absolute terms

755 $\qquad u(x_i) -$ uncertainty in fractional terms

756 3. Compute sensitivity of y to changes in x_i, i.e. partial differentiation for each input.
757   The absolute and fractional inputs are given by:

$$c_i = \frac{\partial y}{\partial x_i} \tag{A-2}$$

$$c_i{}^* = \frac{\partial y}{\partial x_i} \cdot \frac{x_i}{y} \tag{A-3}$$

758 4. A combination of the uncertainties for a set of uncorrelated inputs is obtained by
759   summation of uncertainties for each input. The absolute and fractional terms are
760   expressed as:

$$u_c(y) = \sqrt{\sum_{i=1}^{n} \left(c_i \cdot u(x_i) \right)^2} \tag{A-4}$$

$$u_c^*(y) = \sqrt{\sum_{i=1}^{n}\left(c_i^* \cdot u^*(x_i)\right)^2} \qquad\qquad \text{(A-5)}$$

761 Uncertainties in the superficial liquid and gas liquid velocities, liquid holdup, pressure
762 gradient and liquid viscosity is described in the following sections together with sample
763 calculation.

A.1.1 Uncertainty in superficial liquid velocity

765 The liquid superficial velocity, V_{SL} is a function of the mass flow rate, $\dot{M}_L$ liquid density, ρ_L
766 and flow area, A. For the purpose of this evaluation, the pipe diameter and hence the flow
767 area will be considered constant. The Coriolis mass flow meter is used to obtain the mass
768 flow rate and liquid density, from the manufacturer's guide, the maximum error in
769 measurement are ±0.5 % and ±0.5 kg/m³ for mass flow rate and liquid density
770 respectively. In evaluating the uncertainty, we follow the steps:

771   1. Determine standard uncertainty of each of the functions based on their respective
772   measurement equipment and confidence level. Assuming a 95.4% confidence
773   level;

$$V_{SL} = \frac{\dot{M}_L}{\rho_L A} = \frac{4\dot{M}_L}{\rho_L \pi D^2} \qquad\qquad \text{(A-1.1)}$$

774   2. Partial derivatives of the inputs, Q_L and ρ_L is given by:

$$\frac{\partial V_{SL}}{\partial \dot{M}_L} = \frac{4}{\rho_L \pi D^2} \qquad\qquad \text{(A-1.2)}$$

$$\frac{\partial V_{SL}}{\partial \rho_L} = -\frac{4\dot{M}_L}{\pi (\rho_L D)^2} \qquad\qquad \text{(A-1.3)}$$

775   3. Combined uncertainty in measurement of the superficial liquid velocity is thus:

776

$$u_c(V_{SL}) = \sqrt{\sum_{i=1}^{n}\left(c_i{}^{*}\cdot u^{*}(V_{SL})\right)^2}$$

$$= \sqrt{\left(u_c{}^{*}(\dot{M}_L)\cdot\frac{\partial V_{SL}}{\partial \dot{M}_L}\right)^2 + \left(u_c{}^{*}(\rho_L)\cdot\frac{-4\dot{M}_L}{\pi(\rho_L D)^2}\right)^2}$$

(A-1.4)

777 Case Study

778 In a test case for the 0.0254 m pipe ID test facility, $V_{SL} = 0.10$ m/s, $\dot{M}_L = 180.5$ kg/h, $\rho_L =$

779 $905.8\ kg/m^3$. As earlier stated, pipe diameter is considered a constant while the

780 uncertainty for ρ_L and $\dot{M}_L$ are as given in the manufacturer's manual. Substituting in the

781 combined uncertainty equation at 95.4 % confidence level, the superficial liquid velocity

782 for this condition is ± 0.54 %. Similar analysis for the electromagnetic flowmeter used for

783 metering slurry showed similar results.

784 Generally the uncertainty in measurement of the V_{SLs} (superficial velocity of water, slurry

785 and oil) showed an uncertainty of $\pm 0.55, 0.50\ and\ 0.50$ % respectively. The uncertainty in

786 measuring the sand loadings was negligible ($\pm 10g$) when compared to the sand loading

787 $(loadings > 1kg)$.

788

Uncertainty in pressure gradient

789

790 Pressure gradient in this work was obtained directly from measurements by the

791 differential and point pressure transducers. Based upon this premise, the uncertainty in

792 the measurements of pressure gradient is sourced directly from the stated uncertainties

793 in the manufacturer's guide. For measurements using the single points and the differential

794 pressure transducers, the uncertainties were given as $\pm 2\ and\ \pm 0.04\%$ for the range of

795 $0 - 6\ barg\ and\ -200\ to\ +200$ mbar respectively.

Uncertainty in liquid viscosity

796

797   The uncertainty in liquid viscosity measurement is obtained from the viscometer supplied

798   by Brookfield. The accuracy of the viscometer is given as $\pm 1\%$ of the full range with a

799   repeatability of $\pm\, 0.2\%$ of the full range.

800